Energy-Based Aeroelastic Analysis of a Morphing Wing

Roeland De Breuker[a], Mostafa Abdalla[a], Zafer Gürdal[a], Douglas Lindner[b]

[a]Department of Aerospace Structures, Delft University of Technology, Kluyverweg 1, 2629HS Delft, The Netherlands;
[b]Department of Electrical and Computer Engineering, 302 Whittemore (0111) Virginia Tech Blacksburg, VA 24061, USA

ABSTRACT

Aircraft are often confronted with distinct circumstances during different parts of their mission. Ideally the aircraft should fly optimally in terms of aerodynamic performance and other criteria in each one of these mission requirements. This requires in principle as many different aircraft configurations as there are flight conditions, so therefore a morphing aircraft would be the ideal solution. A morphing aircraft is a flying vehicle that i) changes its state substantially, ii) provides superior system capability and iii) uses a design that integrates innovative technologies. It is important for such aircraft that the gains due to the adaptability to the flight condition are not nullified by the energy consumption to carry out the morphing manoeuvre. Therefore an aeroelastic numerical tool that takes into account the morphing energy is needed to analyse the net gain of the morphing. The code couples three-dimensional beam finite elements model in a co-rotational framework to a lifting-line aerodynamic code. The morphing energy is calculated by summing actuation moments, applied at the beam nodes, multiplied by the required angular rotations of the beam elements. The code is validated with NASTRAN Aeroelasticity Module and found to be in agreement. Finally the applicability of the code is tested for a sweep morphing manoeuvre and it has been demonstrated that sweep morphing can improve the aerodynamic performance of an aircraft and that the inclusion of aeroelastic effects is important.

Keywords: Morphing wing, Aeroelastic Analysis, Generic Analysis Tool, Actuator Energy

Nomenclature

$\mathbf{A}$	Aerodynamic sensitivity matrix
$\mathbf{B}$	Transformation matrix
E_m	Morphing energy
$\mathbf{f}$	Global force vector
$\mathbf{f}_\ell$	Local force vector
$\mathbf{f}_a$	Global aerodynamic force vector
$\mathbf{f}_w$	Force vector containing the weight distribution
$\mathbf{f}_\alpha$	Force sensitivities with respect to α
$\mathbf{f}_{ex}$	Global external force vector
$\mathbf{K}$	Global stiffness matrix
$\mathbf{K}_\ell$	Local stiffness matrix
$\mathbf{K}_s$	Spring stiffness matrix
$\mathbf{K}_t$	Tangential stiffness matrix
$\mathbf{M}_a$	Actuation moment vector
$\mathbf{p}$	Global degrees-of-freedom
$\mathbf{p}_0$	Initial guess for the iteration
$\mathbf{p}_\ell$	Local degrees-of-freedom

Further author information: (Send correspondence to Roeland De Breuker)
Roeland De Breuker: E-mail: r.debreuker@tudelft.nl, Telephone: +31 (0)15 278 5627
Mostafa Abdalla: E-mail: m.m.abdalla@tudelft.nl, Telephone: +31 (0)15 278 5627
Zafer Gürdal: E-mail: z.gurdal@tudelft.nl, Telephone: +31 (0)15 278 2093
Douglas Lindner: E-mail: lindner@vt.edu, Telephone: +1 (540) 231 4580

Modeling, Signal Processing, and Control for Smart Structures 2007, edited by Douglas K. Lindner
Proc. of SPIE Vol. 6523, 652308, (2007) · 0277-786X/07/$18 · doi: 10.1117/12.716731

$\mathbf{p}_\alpha$	Degrees-of-freedom augmented with α
$\Delta\mathbf{p}$	Displacement increment
q	Dynamic pressure
$\mathbf{u}_i$	Global displacements of the ith node
$\bar{u}$	Beam element elongation
V_i	Internal virtual work
α	Angle of incidence
Γ_i	Vortex strength of the ith aerodynamic panel
$\boldsymbol{\theta}_i$	Global rotations of the ith node
$\boldsymbol{\vartheta}_i$	Local rotations of the ith node
λ	Load parameter

1. INTRODUCTION

Due to the often conflicting requirements, which for instance can be very unlike requirements like loiter and high-speed dash, in an aircraft's mission, designers have to make compromises regarding wing layout which compromises aircraft performance. For each segment of the mission, there exists an ideal shape of the wing for optimal performance, and it is therefore advantageous if the wing can conform to all of these shapes. Morphing wings aim to adapt the wing shape to mission requirements enabling the aircraft to fly a multi-role mission optimally. Interest in morphing technology has increased substantially over the past decade. The Defense Advanced Research Projects Agency (DARPA) has defined a morphing aircraft as an aircraft that i) changes its state substantially, ii) provides superior system capability and iii) uses a design that integrates innovative technologies.[1]

Considerable effort has been spent on the analysis of morphing structures, including aeroelastic effects. General planform wings with morphing airfoils are considered[2–4] as well as with variable span.[5] Aeroelastic analysis of folding wings, motivated by the Lockheed Marting Folding Wing concept, was carried out in.[6–10] These analyses range from investigations of the impact of folding angles, hinges, and other design parameters[6,7] to nonlinear studies (in terms of hinge nonlinearities[8]) and multibody dynamic analysis.[9,10]

For optimisation studies of morphing wings fast analysis of morphing energy requirements is essential. Actuation power and added weight required to perform morphing manoeuvres are compared to the aerodynamic/performance gains to assess whether overall performance improvement is possible or not. The optimization of morphing wings for improved performance and minimum actuator energy is carried out by Prock *et al.*[11] Other optimization efforts have been carried out in the field of combined span/airfoil optimisation,[12] combined aspect-ratio/sweep optimisation,[13] or optimisation for pull-up manoeuvres.[14]

Optimisation studies related to the structural design of morphing concepts have also been reported in the literature. Cellular trusses have been designed and optimised with actuators for the NextGen Batwing concept[15] and with tendons for wing shape change in general.[16] Topology optimisation of smart actuator placement using genetic algorithms[17] and the topology optimisation of wing skin thicknesses, spar thicknesses, and flap deflections of morphing wings for aeroservoelastic concepts.[18] Multilevel variable fidelity optimisation techniques for morphing structures are also investigated.[19]

As described in the literature above, substantial research has been conducted regarding analysis, design and optimisation of morphing wings. There are three main categories to which this extensive body of research can be divided: i) the first category is defining individual optimal configurations for specific segments of a mission with conflicting requirements, ii) the second direction is the design of particular morphing concepts with special emphasis on the underlying actuation, and iii) the third category studies in detail the mechanics of particular morphing manoeuvres such as sweep change or folding. Therefore, there seems to be a need for an analysis and optimisation tool for morphing wings that allow morphing to any arbitrary shape in three dimensions while allowing the hinge or flexible locations to be variable and simultaneously taking into account aerodynamics, structural response, and actuation energy into account.

The current paper focusses on the aeroelastic analysis of complete morphing wings incorporating morphing actuator energy. An aeroelastic analysis program, Proteus, is developed. The program integrates a 3D co-rotational structural beam model with a simplified aerodynamic model based on Prandtl's lifting line theory.

The actuator energy is taken into account by applying morphing actuation moments to the beam nodes, which are equipped with a spring to simulate the straining of the skin of the structure.

The rest of the paper is organised as follows. First, the objectives of the analysis are laid out and the problem precisely formulated. This is followed by sections on the structural model, the aerodynamic model, and the details aeroelastic analysis algorithm. The result section follows including verification against commercial finite element analysis and representative results for a case study maximising lift to drag ratio using sweep morphing is presented to demonstrate the capability of the developed code. Finally, conclusions are presented.

2. PROBLEM FORMULATION

Currently two practical morphing wing concepts are under consideration and scaled models have been developed to the flight demonstration stage. These are the Lockheed Martin Folding Wing concept and the NextGen Batwing concept. These two concepts raise the interesting question of finding a more general setting of the problem to allow for comparing different strategies of changing the wing span and/or planform shape. Therefore, a computationally efficient morphing wing analysis and optimisation tool is needed, which allows general morphing in three dimensions. It is also desirable to keep the modelling level simple for use in conceptual design studies.

Morphing wings are structures that by definition exhibit large changes in shape which necessitates a geometrically nonlinear structural model. The wing should be able to fold/sweep/twist in any arbitrary direction at potentially multiple arbitrary locations along the wing span. Furthermore, it is important to consider the interactions between structural deformations, aerodynamics, and morphing actuation. For example, it would be certainly desirable for the aerodynamic loads to assist rather than oppose the morphing deformations.

A morphing wing structure is modelled using three-dimensional nonlinear beam elements. A local linear beam element is used, and large displacement and rotations are accounted for by using an element independent co-rotational framework. Each node has the standard six degrees of freedom. Additional rotational degrees of freedom are introduced to allow for slope discontinuity at nodes. This slope discontinuity allows the possibility of finite sweep/fold angles at any node. A 3D rotational spring, connected at each node, simulates the presence of a hinge. The spring stiffness models the strain energy stored in the skin due to shape change. Arbitrary forces and moments can be applied at each node. These include both aerodynamic loads and actuation moments.

The structural model is coupled to an aerodynamic vortex model based on lifting line theory. This simplified incompressible aerodynamic model allows fast calculation of the circulation while producing accurate trends. Moreover, it can be extended to a compressible model. Since the large deformations of a morphing structure can yield large angles of incidence, these are accounted for in the aerodynamic model. Both the structural and aerodynamic models use the same discretisation, so the nodal aerodynamic forces can be applied as discrete forces on the beam model directly. Tracing the nonlinear equilibrium path is attained by using the Newton-Raphson method.

3. STRUCTURAL MODEL

The structural model consists of linear beam elements in a three-dimensional co-rotational framework. The benefit of using such a framework instead of using nonlinear finite elements is the fact that the local rotations of the beam are known, which comes in handy to derive the aerodynamic mesh from the structural one. This facilitates the analysis of aerodynamic forces and moments considerably (see section 4).

The local beam element formulation is a linear shear-flexible element. The beam elements are connected with flexible rotational springs. In the following, first the local beam model is explained, followed by the co-rotational formulation and the beam connectivity.

3.1. Local Beam Formulation

The local beam element is based on the element of Goyal and Kapania.[20] The element has 22 degrees of freedom and five nodes (four equally-spaced nodes with one additional node in the middle of the beam). The beam allows for shear flexibility and reduces exactly to the standard Hermitian beam element in the limit of high slenderness ratio. The DOFs corresponding to the interior nodes are statically condensed leading to a

12×12 element stiffness matrix. This element has been designed for the modelling of fibre-reinforced laminated composite structures allowing for arbitrary material coupling.

As an input, the beam element accepts the full anisotropic 6×6 beam section stiffness matrix. For instance results from the Variational Asymptotical Beam Sectional Analysis (VABS)[21] can be used. VABS claculates the beam section stiffness matrix for an arbitrary 2D composite cross-section giving a fully populated beam stiffness matrix.

3.2. Co-rotational Framework

The co-rotational approach converts local element forces from the local to global frames. The essential part of the co-rotational formulation is the definition of a local element frame and defining the local element degrees of freedom with respect to that frame. The formulation used in this paper is adopted from Battini and Pacoste.[22]

The global nodal degrees of freedom for the co-rotational element are the displacements of the nodes in the global coordinate system and two rotation vectors describing the rotations between the undeformed and deformed configurations.

$$\mathbf{p} = \begin{bmatrix} \mathbf{u}_1^T & \boldsymbol{\theta}_1^T & \mathbf{u}_2^T & \boldsymbol{\theta}_2^T \end{bmatrix}^T . \tag{1}$$

The local degrees of freedom are extracted from the global degrees of freedom as:

$$\mathbf{p}_\ell = \begin{bmatrix} \bar{u} & \boldsymbol{\vartheta}_1^T & \boldsymbol{\vartheta}_2^T \end{bmatrix}^T \tag{2}$$

where $\bar{u}$ is the change of element length between the current and initial configurations,

$$\bar{u} = L - L_0, \tag{3}$$

and the vectors $\boldsymbol{\vartheta}_i$ are the nodal rotation vector resolved in the local element frame.

The local element forces are obtained from the linear relation:

$$\mathbf{f}_\ell = \mathbf{K}_\ell \cdot \mathbf{p}_\ell \tag{4}$$

and the global load vector and stiffness matrix are obtained using the definition of the co-rotational element frame. The local degrees-of-freedom $\mathbf{p}_\ell$ are a function of the global ones $\mathbf{p}$:

$$\mathbf{p}_\ell = \mathbf{p}_\ell(\mathbf{p}) \tag{5}$$

In order to get an expression for the global force vector, the expressions for the internal virtual work, V_i, in terms of local and global coordinates is equated:

$$V_i = \delta\mathbf{p}_\ell \mathbf{f}_\ell = \delta\mathbf{p}\mathbf{f} \tag{6}$$

from which a direct relation between the two force vectors can be derived:

$$\mathbf{f} = \mathbf{B}^T \mathbf{f}_\ell \tag{7}$$

Taking variations of the latter equation gives the relation between local and global stiffness matrix:

$$\mathbf{K} = \mathbf{B}^T \mathbf{K}_\ell \mathbf{B} + \frac{\partial \mathbf{B}}{\partial \mathbf{p}} : \mathbf{f}_\ell \tag{8}$$

Derivation and expressions for the transformation matrix $\mathbf{B}$ can be found in Battini and Pacoste.[22]

3.3. Beam Connectivity

Each beam element is connected to its neighbour via a rotational spring. This yields nine DOFs per node (three displacements and six rotations). Every node is equipped with three torsion springs (yielding a spring stiffness matrix $\mathbf{K}_s$). This allows the representation a rigid connection (infinite spring stiffness), a hinge (zero spring stiffness), and semi-flexible hinges (finite value of the spring stiffness). Actuation moments, composing the actuation moment vector $\mathbf{M}_a$, can be applied to each spring location.

This particular setup allows the analysis of the morphing energy requirement E_m associated with a certain morphing manoeuvre:

$$E_m = \mathbf{M}_a \cdot \vartheta = \frac{1}{2}\mathbf{K}_s \vartheta \vartheta^T \tag{9}$$

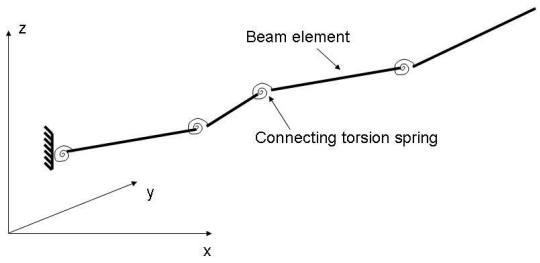

Figure 1. Cantilevered wing built up from hinged beam elements

4. AERODYNAMIC MODEL

The prediction of the aerodynamic performance of a wing is a fairly complex problem and can be modelled with any degree of sophistication. At the lowest level of complexity, strip aerodynamic theory can be used.[23,24] At the higher end an Euler or Navier-Stokes solver can be used. For a coupled aeroelastic problem such as a morphing wing, it is important to match the level of modelling of structures and aerodynamics. For the adopted structural model using beam elements, it is reasonable to use a one-dimensional aerodynamic model such as lifting line theory to predict the aerodynamic loads.[25–27] When a better aerodynamic model is warranted, two-dimensional panel methods such as the vortex lattice method[18,28] can also be used.

A one dimensional vortex-based method is implemented following Katz and Plotkin.[29,30] The basic idea is that a finite wing is represented by a set of n linearly added vortex lines each with strength Γ_i. Each vortex extends downstream to infinity according to Helmholtz' theorem. Each individual vortex is located on an aerodynamic panel at the quarter chord point and induces a downwash speed at the three-quarter chord point on each panel. Flow tangency condition demands zero normal flow on the airfoil and, as such, the unknown vortex strengths are calculated.

The coordinates aerodynamic panels are linked to the structural element geometry. Each structural beam element has an element fixed frame (see figure 2) and the node locations are known as well as the local rotations per node (because of the co-rotational framework). From these parameters, the two-dimensional aerodynamic mesh can be deducted from the one-dimensional beam element. Each beam element can contain multiple aerodynamic panels. In order to achieve this, the nodal rotations are linearly interpolated per beam element.

The lift and induced drag forces are calculated from the vortex strength distribution over the wing. An estimate for the viscous drag is made based on the 2D lift-drag polar, which are reported for all the standard NACA airfoils. The induced and viscous drag added linearly give the total drag. The aerodynamic forces are assumed to act at the quarter chord point of each aerodynamic panel in the direction of the flow (lift) and perpendicular to the flow (drag). The aerodynamic moment is then equal to the product of the lift and the distance between the quarter chord point and the location of the shear centre of the structure.

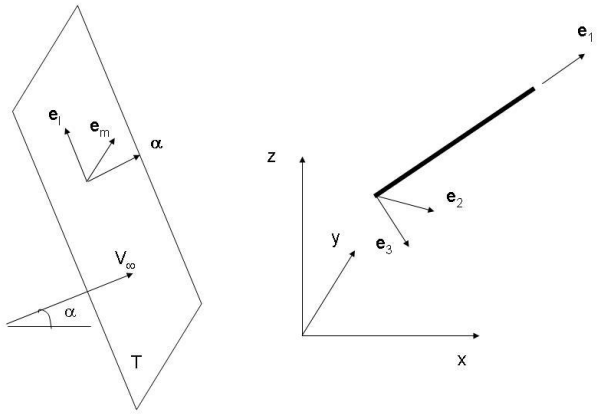

Figure 2. Structural and aerodynamic reference frames

The vector directions of lift, drag and moment forces are linked to the structural element frame. The panel normal is along the direction $\mathbf{e}_3$. The drag force acts along the free-stream velocity vector $\boldsymbol{\alpha}$:

$$\boldsymbol{\alpha} = [\cos(\alpha) \;\; 0 \;\; \sin(\alpha)]^T \tag{10}$$

where α is the angle of incidence. The global vector along which the aerodynamic moment acts, $\mathbf{e}_m$, lies in the plane perpendicular to $\boldsymbol{\alpha}$, usually referred to as the Trefftz plane, and is defined as the projection of the vector $\mathbf{e}_1$ on the Trefftz plane.

$$\mathbf{e}_{1,p} = \mathbf{e}_1 - (\mathbf{e}_1 \cdot \boldsymbol{\alpha}) \cdot \boldsymbol{\alpha} \tag{11}$$

$$\mathbf{e}_m = \frac{\mathbf{e}_{1,p}}{\|\mathbf{e}_{1,p}\|} \tag{12}$$

Finally the vector along which the lift force is to be decomposed, $\mathbf{e}_l$, is perpendicular to both $\boldsymbol{\alpha}$ and $\mathbf{e}_m$:

$$\mathbf{e}_l = \boldsymbol{\alpha} \times \mathbf{e}_m \tag{13}$$

When all the aerodynamic forces and moments are decomposed along their appropriate vectors in the global frame, they are converted to statically equivalent nodal forces to construct the global aerodynamic force vector $\mathbf{f}_a$.

5. STATIC AEROELASTICITY

In the present study, only static aeroelastic effects are considered. To be more specific, deformation under the displacement dependent aerodynamic loads is considered. The discrete equilibrium equations are,

$$\mathbf{f}(\mathbf{p}) = \mathbf{f}_{ex}(\lambda) + \mathbf{f}_a(\mathbf{p}, \alpha, q) \tag{14}$$

where $\mathbf{f}$ is the vector of internal forces that depend on the vector of global degrees-of-freedom $\mathbf{p}$, $\mathbf{f}_{ex}$ the external forces that depend on a load parameter λ, and $\mathbf{f}_a$ the aerodynamic forces which depend on the degrees-of-freedom $\mathbf{p}$, the angle of incidence α and the dynamic pressure q.

When significant nonlinearities are involved, it is customary to trace the response as function of the load parameter λ. In order to determine the equilibrium position at a certain intermediate value for the control parameter an initial guess $\mathbf{p}_0$ is made for the displacement field (usually using a prediction based on the last converged step), then the exact equilibrium displacements are found using the Newton-Raphson method.[31]

Assume that the dynamic pressure q is the only control parameter, the displacement increment $\Delta\mathbf{p}$ is determined from:

$$\left(\mathbf{K}_t(\mathbf{p}_0) - \mathbf{A}(\mathbf{p}_0, q)\right) \Delta\mathbf{p} = \mathbf{f}_{ex} - \mathbf{f}(\mathbf{p}_0) + \mathbf{f}_a((\mathbf{p}_0), q) \tag{15}$$

where $\mathbf{K}_t$ is the tangential stiffness matrix and $\mathbf{A}$ the aerodynamic sensitivity matrix. This matrix contains the changes in aerodynamic loads with the displacement field $\mathbf{p}$. This way, the increment is determined and added to the initial guess until convergence is obtained. An overview of the iteration loops is given in figure 3.

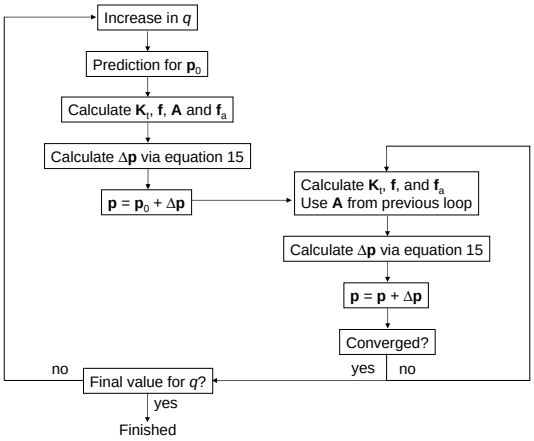

Figure 3. Overview of the two interlaced iteration loops

An analogous procedure holds if the control parameter shows up in the external force vector.

For static performance, the final trimmed state of the aircraft is of interest, not the detailed dynamics of morphing. This trimming condition introduces an additional degree-of-freedom, namely the angle of incidence α. This will augment the DOF vector:

$$\mathbf{p}_\alpha = \begin{bmatrix}\mathbf{p}^T & \alpha\end{bmatrix}^T \tag{16}$$

Therefore equation 15 changes to:

$$\left[\mathbf{K}_t(\mathbf{p}_0) - \mathbf{A}(\mathbf{p}_0, q_{trim}) \;\; \mathbf{f}_\alpha\right] \Delta\mathbf{p}_\alpha = \mathbf{f}_w - \mathbf{f}(\mathbf{p}_0) + \mathbf{f}_a(\mathbf{p}_0, q_{trim}) \tag{17}$$

where $\mathbf{f}_\alpha$ contains the sensitivities of the aerodynamic forces with respect to the angle of incidence α and $\mathbf{f}_w$ is the vector containing the weight distribution of the aircraft and the wing.

6. PROTEUS: FAST AEROELASTIC MORPHING WING ANALYSIS TOOL

The code developed for the fast analysis of morphing wings incorporating aeroelastic effects and actuator energy is called Proteus*. The data flow through the program is explained, and highlighted in figure 4. As an input, the nodal locations of the beam elements, which build up the wing, are given, together with other structural properties such as the chord length at each node, the material stiffness properties at each node and the beam orientation in the global coordinate system. The deformations are zero initially. With this information, the aerodynamic mesh is calculated, based on the number of panels required on each beam element. Using this mesh and other input properties such as flow velocity, angle of attack, and air density, the aerodynamic forces and moments are calculated using the lifting line theory (see section 4). The change of these forces and moments with the global structural displacements, the aerodynamic sensitivities, are calculated using the Matlab Automatic Differentiation toolbox (MAD) for Matlab® by Forth.[32] If a trimming condition is required, the sensitivities of the aerodynamic forces with respect to the angle of attack are also calculated using this technique (see equation 17). All the aerodynamic forces are transferred to the global coordinate system afterwards. The structural displacements, together with the material stiffnesses, are also used to calculate the local force vector and stiffness matrix of each element (see section 3.1). Then they are translated to the global coordinate frame and the system stiffness matrix is composed (see section 3.2). With all the forces and stiffnesses -structural and aerodynamic- the incremental displacements are calculated, based on equation 15 or 17, dependent whether the trimming condition is required. When the incremental displacements are added to the total displacement, convergence is checked. If convergence is not satisfied, the new displacements are added to the structural coordinates and the iteration loop is continued.

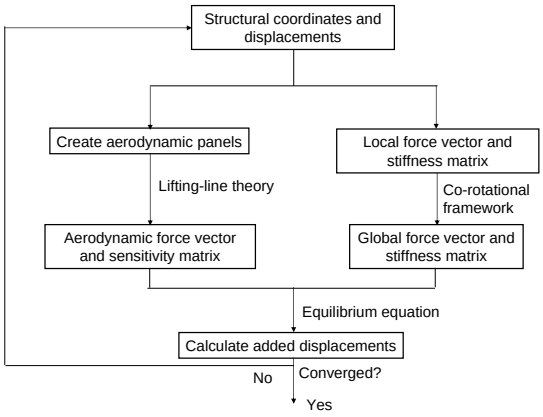

Figure 4. Flow chart of the Proteus program

The aeroelastic results of Proteus are validated against results obtained using NASTRAN Aeroelasticity Module. As a test wing, a simple unswept rectangular wing with a span of 8 m and a chord of 1 m at an angle of incidence $\alpha = 5°$is selected. The flow velocity is 50 m/s. This velocity causes a deformation which is large, but does not trigger the geometrical nonlinearities. The results are shown in figure 5.

It is clear that the results are acceptable (tip displacement within 1 %), although the displacements are not small. This implies that we can put confidence in the structural, aerodynamic and coupling codes.

7. RESULTS AND DISCUSSION

A test case is created to first of all test the functioning of the Proteus code and secondly the concept of sweep morphing in general. An aircraft, having a rectangular wing box, with the properties listed in table 1 is flying in trimmed condition at an airspeed of 64.5 m/s. The sweeping of the wing is carried out at the wing's root,

*Greek mythological god who can change his shape.

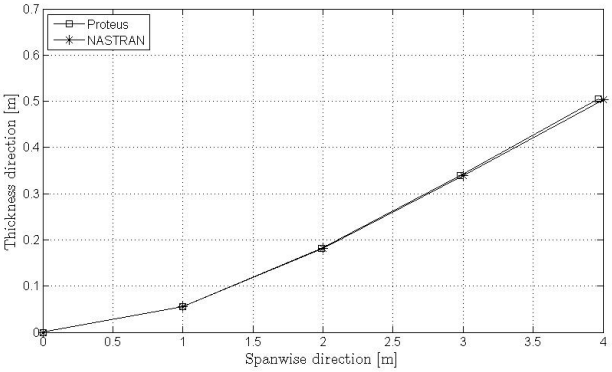

Figure 5. Aeroelastic deflection validation for 50 m/s

where a spring is attached and an actuation moment is applied. The spring stiffness is a discrete model for the distributed skin stiffness of the wing. This is a clear distinction with a rigidly swept wing like the F14. The maximum sweep angle in the analysis is determined by the associated angle of attack. If that angle crosses the maximum angle of attack of 25° in order to keep the aircraft level, the sweeping is stopped.

Table 1. Test case aircraft properties

Weight	20,000 N
Span	10.0 m
Chord	1.6 m
Spring stiffness	1,750 N/m
Box height	100 mm
Box web thickness	2.5 mm
Box width	500 mm
Box flange thickness	5.0 mm

The results presented are the lift to drag ratio (figure 6), the actuation moment applied to perform the sweeping manoeuvre (figure 7) and the change of angle of attack (figure 8) with increasing sweep angle.

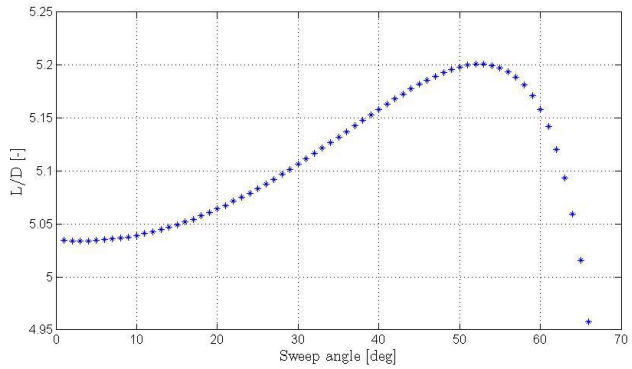

Figure 6. Lift to drag ratio versus sweep angle

It is evident from this figure that the aerodynamic performance in terms of lift to drag ratio first increases with increasing sweep angle until it reaches a certain maximum at a sweep angle of approximately 55°, after

which it decreases again. It is shown that sweeping the wing can increase the aerodynamic performance.

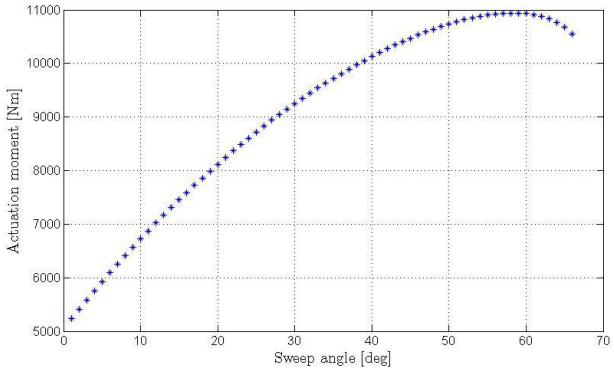

Figure 7. Actuation moment versus sweep angle

The actuation moment increases first almost linearly until a sweep angle of approximately 60° because the spring which is located at the root is strained, thus storing more energy. But after the aforementioned value of the wing sweep angle, the required actuation moment decreases again because the increased drag due to the increased angle of attack "helps" the wing to sweep. This demonstrates the importance of incorporating structures, aerodynamics and actuator energy into the analysis.

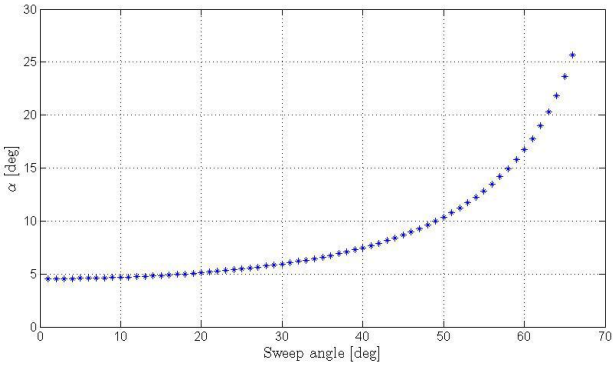

Figure 8. Angle of attack versus sweep angle

Finally the angle of attack increases exponentially with increasing sweep angle. This is because the wing area reduces with increasing sweep angle and hence the angle of attack needs to make up for the lost wing area to keep the aircraft level. At approximately 66° sweep angle, the aircraft reaches a very large angle of attack, which is a measure for the fact that the aircraft stalls.

8. CONCLUSIONS

In this paper an aeroelastic code for morphing wing analysis is presented. The program incorporates a structural beam element code in a co-rotational framework coupled to a lifting-line aerodynamic model via a Newton-Raphson iteration method. It also allows morphing in any arbitrary direction in a three-dimensional space as well as the evaluation of the morphing energy associated with the morphing manoeuvre. The code is validated against results from NASTRAN Aeroelasticity Module and provides satisfactory results. Finally the program is used in a test case of a sweep morphing wing. It has been demonstrated that sweep morphing in certain cases indeed can improve the aerodynamic performance in terms of lift-to-drag ratio.

Future work will consist of the embedding of this code in an optimisation routine to determine the optimal morphing manoeuvre subjected to certain constraints and objectives. Also a more refined aerodynamic model is aimed for in order to deal with transonic and supersonic flows. Finally the work will be extended to a dynamic structural model coupled to an unsteady aerodynamic model.

ACKNOWLEDGMENTS

The authors would like to warmly acknowledge the contribution of Dr. Battini for putting his Matlab® code for the co-rotational framework at disposal. Furthermore Dr. Forth is acknowledged cordially for the use of his Matlab® toolbox on Automatic Differentiation. Finally the authors would like to thank Dr. Sanders and Mr. Reich of the AFRL for their valuable contribution and suggestions.

REFERENCES

1. J. Wilson, "Morphing uavs change the shape of warfare." Aerospace America, February 2004.
2. F. Gern, D. Inman, and R. Kapania, "Structural and aeroelastic modeling of general planform wings with morphing airfoils," *AIAA Journal* **40**, pp. 628–637, April 2002.
3. F. Gern, D. Inman, and R. Kapania, "Computation of actuation power requirements for smart wings with morphing airfoils," in *Proceedings of the 43rd AIAA/ASME/ASCE/AHS/ASC Structures, Structural Dynamics and Materials Conference*, April 2002.
4. F. Gern, D. Inman, and R. Kapania, "Computation of actuation power requirements for smart wings with mophing airfoils," *AIAA Journal* **43**, December 2005.
5. J.-S. Bae, T. Seigler, and D. Inman, "Aerodynamic and aeroelastic considerations of a variable-span morphing wing," in *Proceedings of the 45th AIAA/ASME/ASCE/AHS/ASC Structures, Structural Dynamics and Materials Conference*, April 2004.
6. D. Lee and T. Weisshaar, "Aeroelastic studies on a folding wing configuration," in *Proceedings of the 46th AIAA/ASME/ASCE/AHS/ACS Structures, Structural Dynamics and Materials Conference*, April 2005.
7. M. Snyder, B. Sanders, F. Eastep, and G. Frank, "Vibration and flutter characteristics of a folding wing," in *Proceedings of the 46th AIAA/ASME/ASCE/AHS/ACS Structures, Structural Dynamics and Materials Conference*, April 2005.
8. D. Lee and P. Chen, "Nonlinear aeroelastic studies on a folding wing configuration with free-play hinge nonlinearity," in *Proceedings of the 47th AIAA/ASME/ASCE/AHS/ASC Structures, Structural Dynamics and Materials Conference*, May 2006.
9. G. Reich, J. Bowman, B. Sanders, and G. Frank, "Develoment of an integrated aeroelastic multibody morphing simulation tool," in *Proceedings of the 47th AIAA/ASME/ASCE/AHS/ASC Structures, Structural Dynamics and Materials Conference*, May 2006.
10. J. Scarlett, R. Canfield, and B. Sanders, "Multibody dynamic aeroelastic simulation of a filding wing aircraft," in *Proceedings of the 47th AIAA/ASME/ASCE/AHS/ASC Structures, Structural Dynamics and Materials Conference*, May 2006.
11. B. Prock, T. Weisshaar, and W. Crossley, "Morphing airfoil shape change optimization with minimum actuator energy as an objective," in *Proceedings of the 9th AIAA/ISSMO Symposium of Multidisciplinary Analysis and Optimization*, September 2002.
12. J. Vale, F. Lau, A. Suleman, and P. Gamboa, "Multidisciplinary design optimization of a morphing wing for and experimental uav," in *Proceedings of the 11th AIAA/ISSMO Multidisciplinary Analysis and Optimization Conference*, September 2006.
13. S. Ricci and M. Terraneo, "Application of mdo techniques to the preliminary design of morphed aircraft," in *Proceedings of the 11th AIAA/ISSMO Multidisciplinary Analysis and Optimization Conference*, September 2006.
14. N. Khot, J. Zweber, D. Veley, K. Appa, and F. Eastep, "Optimization of a flexible composite wing for pull-up maneuver with internal actuation," in *Proceedings of the 42nd AIAA/ASME/AHS/ASC Structures, Structural Dynamics and Materials Conference*, April 2001.

15. T. Johnson, M. Frecker, J. Joo, M. Abdalla, B. Sanders, Z. Gurdal, and D. Lindner, "Nonlinear analysis and optimization of diamond cell morphing wings," in *Proceedings of the 2006 ASME International Mechanical Engineering Congress and Exposition*, 2006.
16. D. Ramrkahyani, G. Lesieutre, M. Frecker, and S. Bharti, "Aircraft structural morphing using tendon actuated compliant cellular trusses," in *Proceedings of the 45th AIAA/ASME/AHS/ASC Structures, Structural Dynamics and Materials Conference*, April 2004.
17. A. Cook and W. Crossley, "Investigation of genetic algorithm approaches for smart actuator placement for aircraft maneuvering," in *Proceedings of the 39th AIAA Aerospace Sciences Meeting and Exhibit*, January 2001.
18. J. Henderson, "Global optimisation methods for aeroservoelastic concepts," in *Proceedings of the 43rd AIAA/ASME/AHS/ASC Structures, Structural Dynamics and Materials Conference*, April 2002.
19. S. Gano, V. Perez, J. Renaud, S. Batill, and B. Sanders, "Multilevel variable fidelity optimization of a morphing unmanned aerial vehicle," in *Proceedings of the 45th AIAA/ASME/AHS/ASC Structures, Structural Dynamics and Materials Conference*, April 2004.
20. V. Goyal and R. Kapania, "A shear-flexible beam element for linear analysis of unsymmetrically laminated beams," in *Proceedings of the 43rd AIAA/ASME/ASCE/AHS/ASC Conference*, April 2002.
21. C. Cesnik and D. Hodges, "Vabs: A new concept for composite rotor blade cross-sectional modeling," *Journal of the American Helicopter Society* **42**(1), pp. 27–38, 1997.
22. J.-M. Battini and C. Pacoste, "Co-rotational beam elements with warping effects in instability problems," *Computer Methods in Applied Mechanics and Engineering* **191**, pp. 1755–1789, 2002.
23. R. Bisplinghoff, H. Ashley, and R. L. Halfman, *Aeroelasticity*, Dover Publications, Inc., New York, 1955.
24. R. Bisplinghoff and H. Ashley, *Principles of Aeroelasticity*, Dover Publications, Inc., New York, 1962.
25. M. Drela, "Integrated simulation model for preliminary aerodynamic, structural and control-law design of aircraft," in *Proceedings of the 40th AIAA/ASME/ASCE/AHS/ASC Structures, Structural Dynamics and Materials Conference*, April 1999.
26. J.-J. Chattot, "Analysis and design of wings and wing/winglet combinations at low speeds," in *Proceedings of the 42nd AIAA Aerospace Sciences Meeting and Exhibit*, January 2004.
27. B. Lawrence, G. Padfield, and P. Perfect, "Flexible uses of simulation tools in an academic environment," in *Proceedings of the AIAA Modeling and Simulation Technologies Conference and Exhibit*, August 2006.
28. M. Abdulrahim and R. Lind, "Using avian morphology to enhance aircraft maneuvrability," in *Proceedings of the AIAA Atmospheric Flight Mechanics Conference and Exhibit*, August 2006.
29. J. Katz and A. Plotkin, *Low-Speed Aerodynamics, Second Edition*, Aerospace Series, Cambridge University Press, 2001.
30. J. Anderson, *Fundamentals of Aerodynamics, second edition*, McGraw-Hill Internation Editions, New York, 1991.
31. M. Crisfield, *Non-linear Finite Element Analysis of Solids and Structures*, vol. 1, John Wiley & Sons Ltd., The Atrium, Southern Gate, Chichester, West Sussex PO19 8SQ, England, 1991.
32. S. Forth and M. Edvall, *User Guide for Mad - a Matlab Automatic Differentiation Toolbox TOMLAB/MAD*, Tomlab Optimization Inc., 855 Beech St 121, San Diego, CA, USA, version 1.4 ed., November 2006.